Development of Stable Iron Oxide Nanoparticles for Dynamic Covalent Surface Functionalization

Xiaoming Miao[1], Niek N. H. M. Eisink[2], Piotr Nowak[1], Meniz Altay[1], Giulia Leonetti[1], Ivana Marić[1], Martin D. Witte[2], Adriaan J. Minnaard[2] and Sijbren Otto[1]*

ABSTRACT

Water dispersed surface-functionalized superparamagnetic iron oxide nanoparticles (SPIONs) have many applications in various fields and especially in biomedical research. The monodispersity and stability of these nanoparticles and the ability to functionalize their surfaces are critical factors for successful applications. Numerous approaches have been developed that aim at stable and monodispersed SPIONs in aqueous solution. Nevertheless, obtaining water-soluble SPIONs that are stable for prolonged periods (i.e. months) remains challenging. Here, a series of ligands was synthesized featuring nitrocatechol as SPIONs anchor and different polar groups for water solubility. We found that nanoparticles coated with zwitterionic ligands were stable for well over two months, which exceeded the stability of analogues containing negatively charged, positively charged or neutral ligands. A choline phosphate-based zwitterionic ligand was further functionalized with an aldehyde group that facilitated facile additional surface functionalization by means of hydrazone chemistry. These results establish SPIONs as a new platform for reversible covalent surface functionalization, opening up new opportunities in systems chemistry and biomedical applications.

Keywords: dynamic covalent chemistry, surface-functionalization; magnetic nanoparticles; hydrazones.

Introduction

Surface-functionalized superparamagnetic nanoparticles have many applications in various fields, especially in biomedical research, including magnetic resonance imaging (MRI) [1 - 4], hyperthermia treatment of tumors [5 - 6], and magnetic separation of biomolecules and directional drug delivery [7 - 8]. Many of these applications place stringent demands on stability and monodispersity of the SPIONs under physiological conditions [9]. Although the preparation of monodisperse SPIONs in organic media is well-established [10 - 12], making SPIONs that exhibit long-term stability in aqueous solution remains challenging. The common strategies for preparing stable SPIONs in aqueous medium make use of ligands that prevent SPIONs from forming aggregates through electrostatic repulsion or steric effects [13 - 17]. For example, *Reimhult* and *Textor* have developed nitrocatechol grafted polymers as stabilizing ligand for SPIONs in aqueous solution [15, 18 - 20]. Also small-molecule spacers carrying charges are commonly applied, as SPIONs coated

*Correspondence: s.otto@rug.nl
[1]Centre for Systems Chemistry, Stratingh Institute for Chemistry, University of Groningen, Nijenborgh 4, 9747 AG Groningen, The Netherlands. (Full list of author information is available at the end of the article.)

with relatively small ligands have a large core/shell ratio which is crucial for magnetic interactions [13]. While several procedures for preparing water soluble SPIONS have been reported, a systematic study comparing the stability of SPIONs coated with different types of polar ligands has not yet

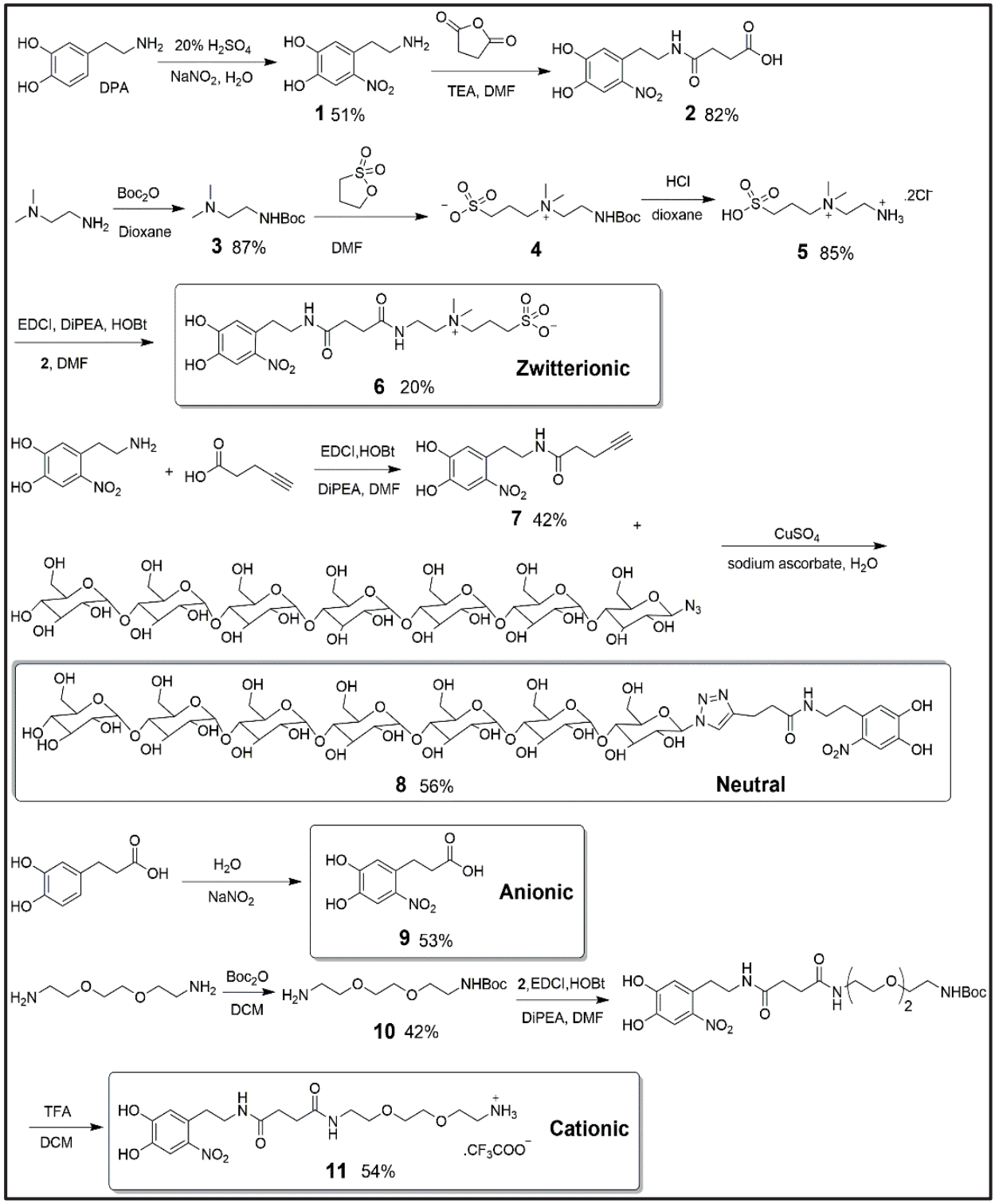

Scheme 1. Structures and synthesis of the zwitterionic, neutral, anionic, and cationic ligands.

been performed.

Here, we designed a set of ligands functionalized with the moiety that is most commonly used as the anchor to the SPIONs surface: a nitrocatechol group. The ligands were further equipped with different groups that were expected to endow them with water solubility, including zwitterionic, neutral, as well as anionic, and cationic ones. The stabilities of SPIONs grafted with these ligands were studied in aqueous solution at different pH values and salt concentrations by dynamic light scattering (DLS). We found that aqueous solutions of sulfobetaine-conjugated zwitterionic ligand-coated SPIONs were remarkably stable, showing no signs of aggregation over a period exceeding two months. Another zwitterionic ligand containing a choline phosphate moiety was then synthesized and equipped with an aldehyde group to enable facile further surface functionalization through reversible covalent hydrazone chemistry. These nanoparticles provide a useful platform for future applications in systems chemistry.

Results and Discussion

Ligand Design and Synthesis

The ligands were designed to contain nitrocatechol for anchoring to the SPION surface and a polar group for water solubility. The choice for the catechol anchor was based on the fact that 3,4-dihydroxyphenylalanine and dopamine (*Scheme 1*) possess a catechol group that has a strong binding affinity for several metal ions [15, 19, 21 – 23]. These catechol ligands play an essential role in the mussel adhesion mechanism [24]. Inspired by these observations, the catechol moiety has become a popular anchor for the functionalization of iron oxide and titanium oxide nanoparticles [15, 25 – 26]. However, catechols are readily oxidized by iron(III) to quinones which results in a loss of affinity for the SPION surface, leading to the aggregation of the SPIONs. Introducing a nitro group on the *ortho*-position of the catechol ring largely prevents catechol oxidation [15, 19].

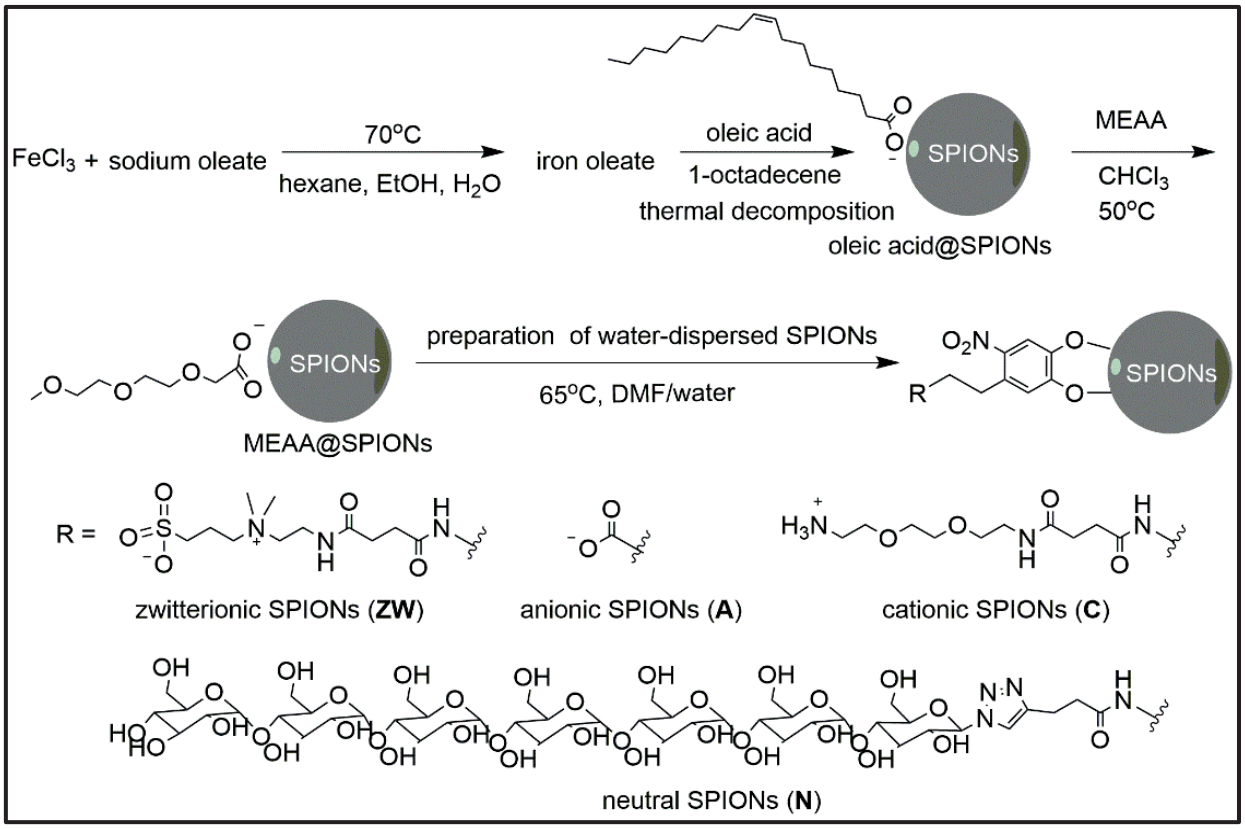

Figure 1. Preparation of different water-dispersed SPIONs.

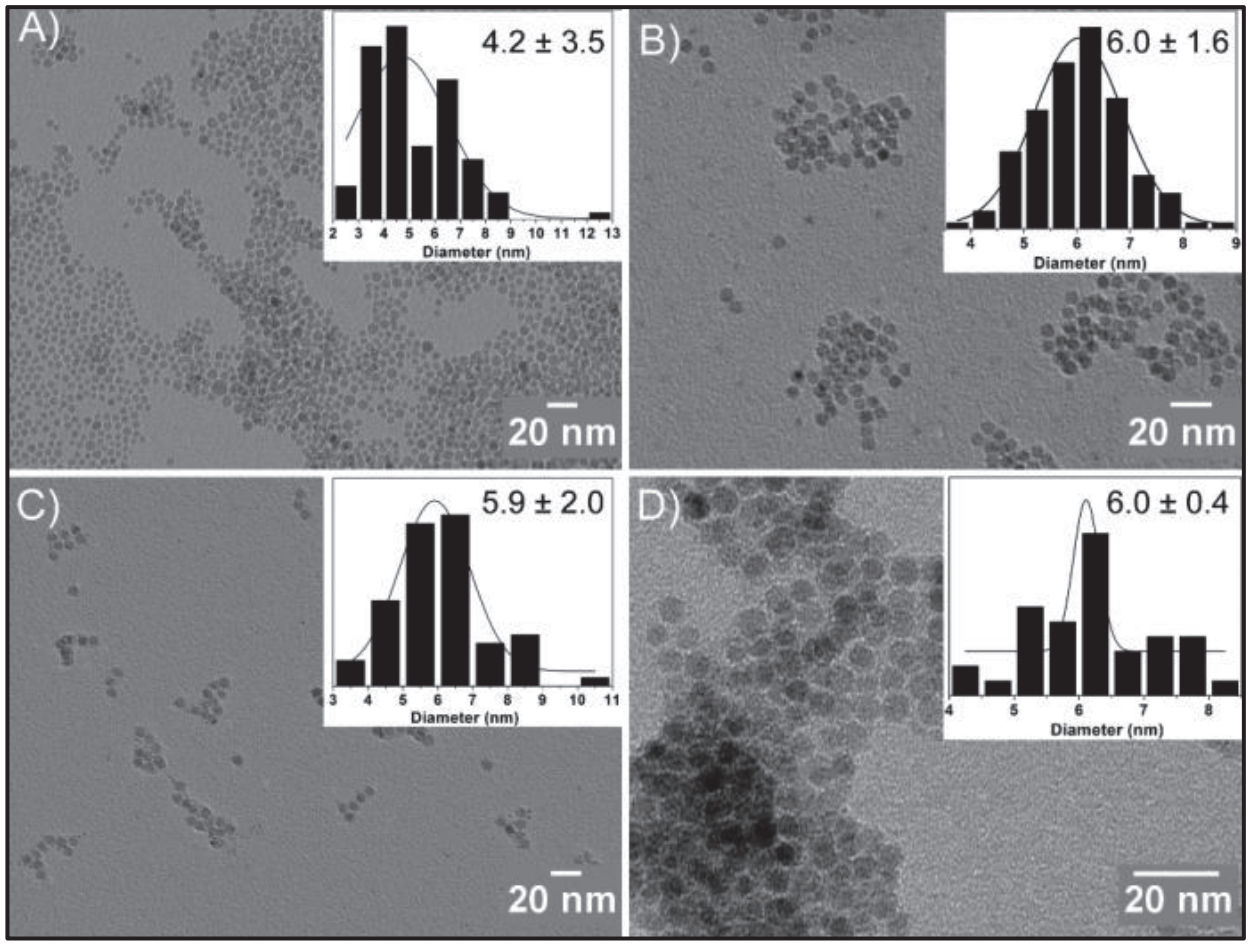

Figure 2. TEM image of *A*) **zwitterionic SPIONs**, *B*) **neutral SPIONs**, *C*) **anionic SPIONs**, **and** *D*) **cationic SPIONs**. The inserts show histograms of the particle diameter as measured by TEM.

Water solubility may be achieved with anionic, cationic, zwitterionic, or neutral ligands. We designed and synthesized ligands to represent each of these four classes (*Scheme 1*). Specifically, we designed the zwitterionic ligand **6** to contain a quaternary ammonium–sulfonate conjugate; the neutral ligand **8** features a biocompatible oligosaccharide [27]. We reasoned that the neutral but large oligosaccharide ligand could potentially stabilize the SPIONs by preventing the exchange of surface ligands with molecules from the environment due to steric hindrance. Similar stabilizing effects of oligosaccharides are often encountered in biological systems, *e.g.*, protein glycosylation can prevent proteases from accessing the peptide backbone, providing resistance to enzymatic degradation [28 - 29]. The anionic ligand **9** contains a carboxylic acid (deprotonated at neutral pH), while cationic ligand **11** features an amine group (protonated at neutral pH).

The synthesis of these four ligands is depicted in *Scheme 1*. First dopamine was nitrated with $NaNO_2$ in the presence of 20% H_2SO_4 and then reacted with succinic anhydride to provide compound **2** as an intermediate for further functionalization. The zwitterionic ligand was synthesized by a ring-opening reaction between tertiary amine **3** and propane-1,3-sultone.

Deprotection of the resulting compound **4** afforded **5**, which was reacted with **2** to yield the desired ligand **6**. Oligomaltose was used as a neutral solubilizing group. β-D-maltoheptaosyl azide was reacted with compound **7** through a Cu-catalyzed click reaction to obtain ligand **8**. Anionic ligand **9** was synthesized by nitration of 3,4-dihydroxyhydrocinnamic acid. Finally, amidation

of monoprotected amine **10** with carboxylic acid **2** and deprotection afforded cationic ligand **11**. Detailed synthetic procedures and characterization of the four ligands are provided in the *Supporting Information*.

The preparation of aqueously dispersed SPIONs is depicted in *Figure 1*. First, oleic acid-stabilized hydrophobic SPIONs were made by the thermal decomposition of iron oleate which was synthesized by an exchange reaction of FeCl3 with sodium oleate [11]. Homogeneous ligand exchange was then applied to obtain water-dispersed SPIONs. Here, a two-step exchange procedure was adopted, because we did not succeed in finding a solvent in which both the oleic acid stabilized SPIONs, and the charged ligands could be dissolved [13]. An intermediate ligand 2-[2-(2-methoxyethoxy)ethoxy]acetate (MEAA) was utilized to exchange the oleic acid attached to the surface of SPIONs. The resulting MEAA-grafted intermediate SPIONs were soluble in a mixture of DMF and water which was a suitable medium for the subsequent exchange with the water-solubilizing ligands. The thus obtained water-dispersed SPIONs were purified by dialysis. The cationic SPIONs aggregated during purification, whereas the other three SPIONs could be dialyzed at least 6 times without any aggregation. All ligand-exchange reactions were conducted in a sonication bath, as magnetic stirring of the nanoparticle dispersions was found to lead to their aggregation.

Characterization of SPIONs

As NMR is difficult for paramagnetic materials the ligand-exchange process was monitored by IR spectroscopy. The IR spectra are shown in *Figure S1*. C-C single bond and C-H vibrations at *ca*. 1470 and 2870 cm^{-1} were observed for oleic acid@SPIONs. After ligand exchange with MEAA, strong absorptions appeared around 1100 and 1200 cm^{-1} which were assigned to C-O single-bond stretching, while the absorption at 2870 cm^{-1} became smaller, in agreement with oleic acid having been substituted by MEAA. For the SPIONs functionalized with the water-solubilizing ligands, absorptions due to C=O and C=C stretching at 1450 to 1650 cm^{-1} were found, together with a C-O single-bond vibration at 1050 cm^{-1}, suggesting that nitrocatechol is present on the surface of the SPIONs. However, it was not possible to quantify the degree of the ligand exchange from the IR spectra. The Fe-O bond around 600 cm^{-1} is excluded in all spectra, since it is extremely strong compared to the other bands and would compromise the resolution of the remaining part of the IR spectrum.

The morphologies and size distributions of SPIONs were characterized by TEM and DLS. The fresh oleic acid@SPIONs are well-dispersed in hexane which is confirmed by the TEM image in *Figure S2*. The water-soluble zwitterionic, neutral, and anionic SPIONs are observed as well-dispersed spherical nanoparticles with diameters around 4 – 7 nm in TEM (*Figure 2*). The hydrodynamic diameters measured by DLS are somewhat larger (*Figure S4*). However, since the inorganic nanoparticle cores are surrounded by a layer of organic material, and (for the ionic ligands) ions and associated water molecules, which give poor contrast in TEM, these results are in good agreement. Cationic SPIONs precipitated during dialysis, leading to large aggregates found both in TEM (*Figure 2*) and DLS (*Figure S4*). The polydispersities measured by DLS for the prepared SPIONs are between 0.2 and 0.3, indicating some degree of aggregation, which is probably inherited from the intermediate MEAA@SPIONs, as MEAA is not a good ligand for stabilizing SPIONs. The SPIONs were not further purified because the number of aggregates was rather low.

The extent of surface coverage of the SPIONs was estimated by thermogravimetric analysis (TGA) [15, 30, 31]. *Figure S3* shows that, as the temperature is increased from 20 to 600 °C, several stages of weight loss occur. We interpret the slowly changing weight at 20 to 200 °C to be caused by evaporation of water. The coated ligands start to be decomposed in the range between 200 and 450 °C.

The corresponding weight decrease in this range amounts to 19, 27, 25, and 24% for zwitterionic, neutral, anionic, and cationic SPIONs, respectively.

Table 1. Characterization details of the four water-dispersed SPIONs.					
SPIONs	Diameter (TEM) (nm)	Ligand density (/nm²)	Diameter (DLS) (nm)	Polydispersity	Zeta-potential (mV)
Zwitterionic	4.2	1.0	11	0.28	-9.8
Neutral	6.0	0.77	29	0.28	-13
Anionic	5.9	2.3	25	0.26	-19
Cationic	6.0	1.5	aggregates	0.35	-4.2

The grafting densities of the ligands were subsequently calculated using *Equation S1*. The coating density together with the average nanoparticle size, polydispersity, and zeta potential are collected in *Table 1*. The number of ligands per unit surface area correlates roughly with ligand size: this number is smallest for the large neutral ligand and largest for the anionic ligand, which is the smallest of all.

Stability Studies

The stabilities of the SPIONs coated with different charged ligands were studied by DLS in aqueous solution at different pH and in the presence of different salts during a period of 70 days. *Figure 3* shows the results after two hours.

As shown in *Figure 3, A*, all of four SPIONs aggregated upon acidification to pH 1, as indicated by the large increase in hydrodynamic size. The zwitterionic SPIONs exhibited the lowest degree of aggregation (mean size of *ca*. 150 nm, while assemblies of around 1 μm were formed by the three other SPIONs). Also, the onset of aggregation upon lowering the pH occurs at a more acidic environment for the zwitterionic SPIONs. The zwitterionic, as well as neutral and anionic SPIONs, are stable for at least two hours above pH 5 with a constant hydrodynamic diameter from pH 5 to pH 13. It is well-established that the interactions between catechol and iron ions are influenced by pH [32 – 34]. At low pH, the protonation of the catechol OH groups hampers their binding to the SPION surface [35]. No experiment was performed at pH > 13, as iron hydroxide precipitates under these strongly basic conditions due to ligand exchange with hydroxide ions.

Next, the stabilities of the SPIONs to different salts were studied, including NaCl (containing only monovalent ions), $MgCl_2$ (featuring a divalent cation), and Na_2SO_4 (containing a divalent anion). As shown in *Figure 3B*, zwitterionic SPIONs are stable to NaCl concentrations as high as 1.0 M. We attribute the slight size increase at high concentration of NaCl to ions doping to the SPION surface through the association between the counterions in the solution [36]. In contrast, the neutral and anionic SPIONs are not able to withstand the high concentration (1 M) of NaCl. The stabilities of SPIONs in salt solutions containing divalent ions are shown in *Figure 3*, *C* and *D*. The SPIONs are relatively stable up to 100 mM Na_2SO_4, while a high concentration (1 M) of this salt induces aggregation of all SPIONs. $MgCl_2$ causes aggregation already at lower concentrations (10 mM). Only the zwitterionic SPIONs remain stable in the presence of 10 mM $MgCl_2$. Mg^{2+} most likely competes with the SPION surface for the ligands by forming magnesium catechol adducts [37]. Note that the cationic SPIONs were already aggregated prior to these experiments. These aggregates did not change in size very much subsequently.

We compared the DLS data of the four SPIONs after 2 h with the corresponding data obtained after 1, 30, and 70 days at different pH values and salt concentrations (*Figures 4* and *5*). Zwitterionic NPs are stable at pH 7 - 13 during the entire period. At pH 1 – 5, they had formed precipitates after 70 days. Interestingly, their size became smaller after 30 days at pH 5 which may be due to ligand exchange with citric acid present in the buffer. Neutral SPIONs slightly aggregated at pH 5 - 9 over time, while anionic SPIONs showed only short-term stability. Anionic SPIONs are stable only at pH 13, presumably as a result of a greater degree of charge repulsion between these

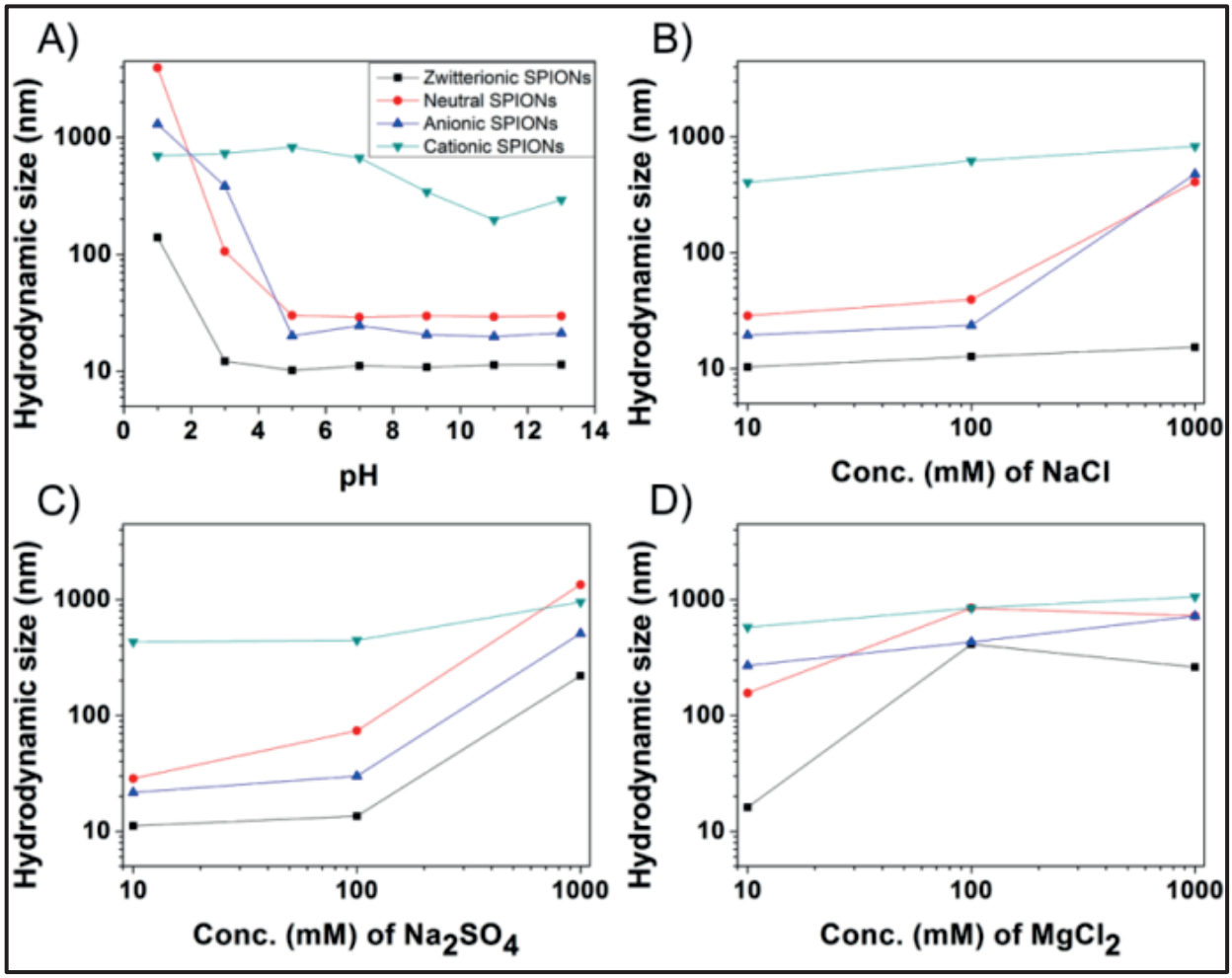

Figure 3. The mean hydrodynamic size (number fraction) of four SPIONs. *A*) At pH 1, 3, 5, 7, 9, 11, and 13, respectively; *B*) in the presence of 10, 100, and 1000 mM NaCl; *C*) in the presence of 10, 100, and 1000 mM of Na_2SO_4; *D*) in the presence of 10, 100, and 1000 mM of $MgCl_2$. All hydrodynamic sizes were measured by DLS at 25 °C after incubation for two hours. *Black squares* represent zwitterionic SPIONs; *red rhombus*: neutral SPIONs; *blue triangle*: anionic SPIONs, and *cyan inverted triangle*: cationic SPIONs. The average size of aggregated samples is only an indicative number that reflects the degree of aggregation.

SPIONs at elevated pH. Cationic SPIONs aggregated during all tests.

In the presence of different salts, zwitterionic SPIONs remain well dispersed even after 70 days, as shown in *Figure 5*, *A*. In contrast, neutral and anionic SPIONs had a aggregated after 70 days as shown in *Figure 5*, *B* and *C* Thus, zwitterionic SPIONs display promising long-term stability compared to the neutral, anionic, and cationic counterparts, which makes them good candidates for further application.

Aldehyde Functionalization and Hydrazone Conjugation

Given that the zwitterionic ligand yields remarkably stable SPIONs, and given that zwitterionic ligands are also reported to minimize nonspecific absorption of the SPIONs, [13] we decided to develop these materials as a platform for further conjugation. We grafted benzaldehyde groups to the surface of the zwitterionic SPIONs, since aromatic aldehydes can react with many nitrogen nucleophiles under mild aqueous conditions to yield imines, hydrazones and oximes. As the benzaldehyde group is quite hydrophobic,

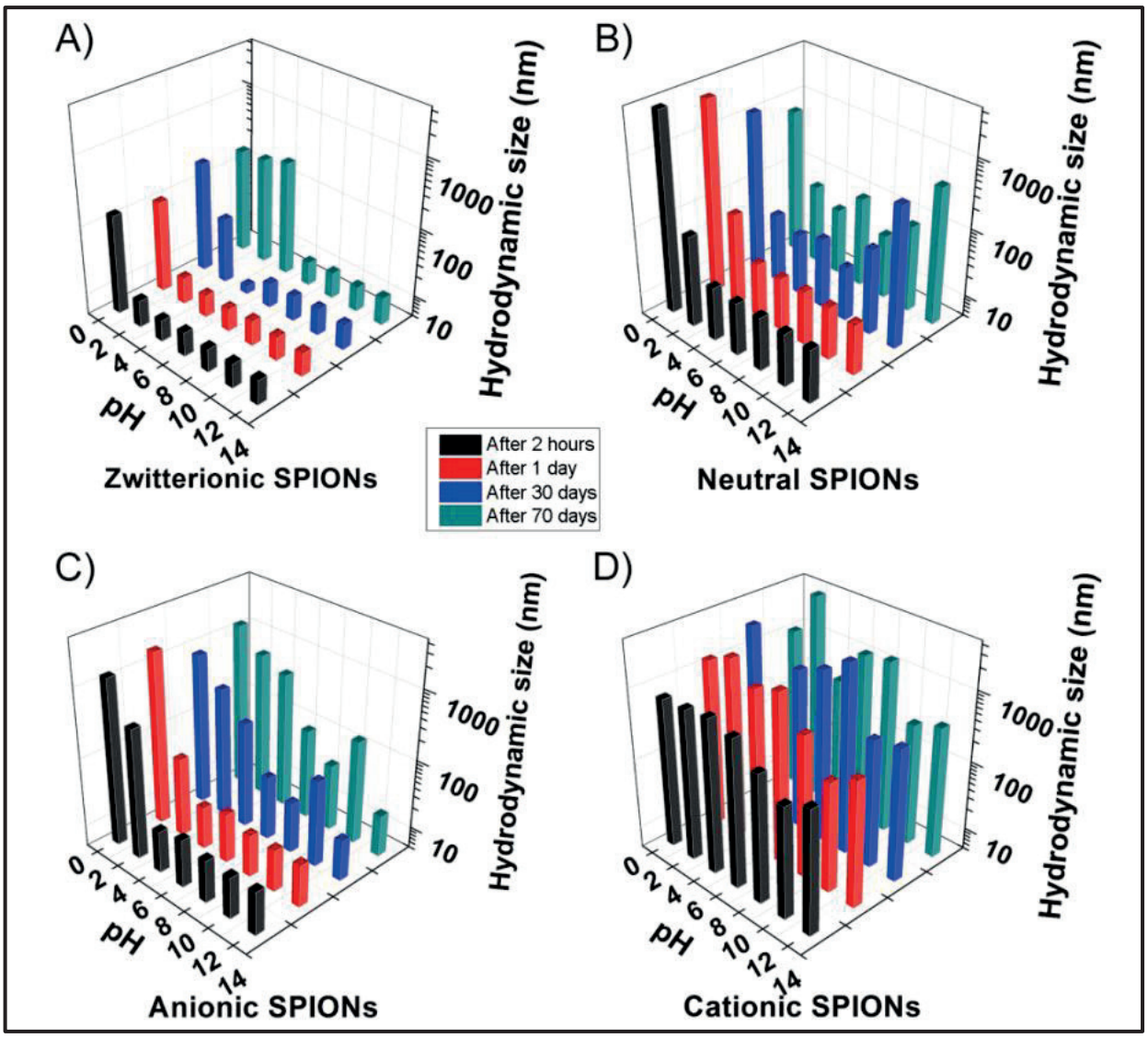

Figure 4. Mean hydrodynamic size (number fraction) of zwitterionic (A), **neutral** (B), **anionic** (C)**, and cationic** (D) **SPIONs at different pH as a function of time.** Hydrodynamic sizes were measured by DLS at 25 °C 2 hours after sample preparation (*black*); after 1 day (*red*); 30 days (*blue*), and 70 days (*cyan*). The average size of aggregated samples is only an indicative number that reflects the degree of aggregation.

obtaining well-dispersed nanoparticles with a high surface coverage of benzaldehydes in aqueous solution puts stringent demands on the design of the ligand [38]. We decided to incorporate the zwitterionic choline phosphate moiety in the ligand [39]. Ligand **14** (*Figure 6, A*) was prepared in four steps, including a phosphorylation and a ring-opening reaction as well as amidation. The overall yield was low partly due to the challenges posed by the EDC-mediated amidation step, which had to be conducted in water-containing solvents to dissolve **13** and to prevent this compound from forming imines. EDC is easily hydrolyzed by water, requiring the use of an excess of EDC, causing its conjugation with one of the hydroxy groups of catechol (*Scheme S1*). It was possible to convert this side-product into the desired ligand **14** through the two-step procedure shown in *Scheme S1*. It was possible to control the aldehyde surface density of the SPIONs by working with different ratios of zwitterionic ligand **6** and zwitterionic aldehyde **14**. We prepared four sets of SPIONs with

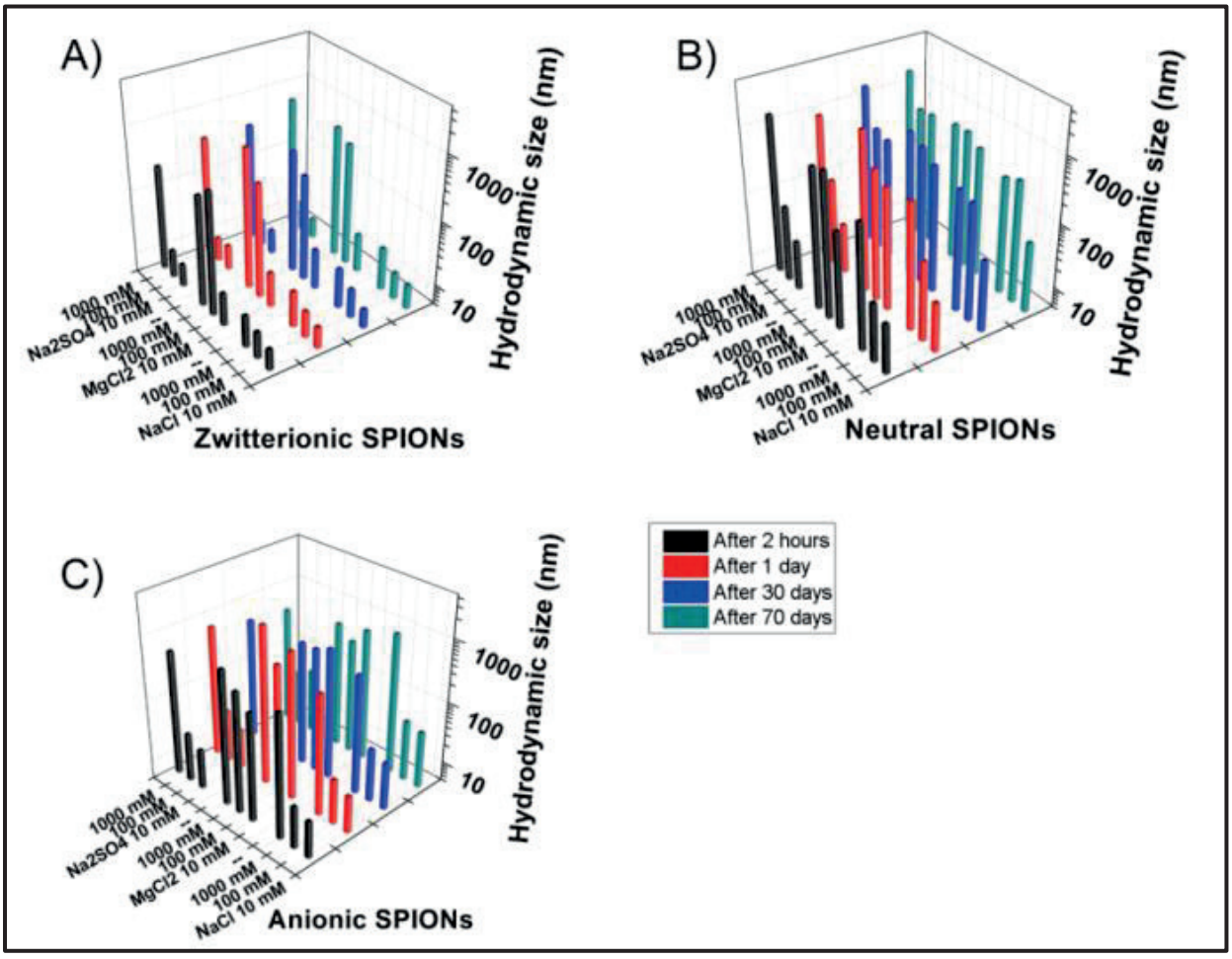

Figure 5. Mean hydrodynamic size (number fraction, measured by DLS at 25 °C) **of zwitterionic** (**A**), **neutral** (*B*), **and anionic** (C) **SPIONs in the presence of different salts at different salt concentration measured 2 hours after sample preparation** (*black*); **after 1 day** (*red*); **30 days** (*blue*), **and 70 days** (*cyan*). The average size of aggregated samples is only an indicative number that reflects the degree of aggregation.

25%, 50%, 75%, and 100% of the aldehyde ligand. The hydrodynamic size was measured by DLS (*Figure S5*), showing that all of these SPIONs were well-dispersed in aqueous solution. This conclusion was confirmed by TEM analysis of the SPION sample prepared from a 1:1 mixture of **6** and **14** (*Figure S6*). All four SPIONs are stable up to 70 days. We also noticed that only a few aggregates formed in the sample of SPIONs coated with 100% **14** after four months' storage. Together with the zwitterionic SPIONs made from **6** only, these samples were characterized by UV, which indicated the presence of the aromatic aldehyde group in **14**, which has a maximum absorption at 270 nm. As shown in *Figure 7*, *A*, the peak at 270 nm increases with increasing fraction of the benzaldehyde ligand. To show that these aldehyde-functionalized SPIONs can be readily functionalized further, we reacted them with the fluorescent hydrazide dye NBD-CO-Hz in the presence of aniline as a catalyst (*Figure 6*, *B*). After purification by centrifugal filtration, the resulting zwitterionic SPIONs were characterized by UV (*Figure 7*, *B*) and fluorescence (*Figure S7*) spectroscopy. The normalized UV spectrum shows a peak around 470 nm which increases as the **14**:**6** ratio increases, which indicates that more NBD molecules become attached to the surface of the SPIONs which have a higher aldehyde coverage. The maximum absorption of NBD shifts from

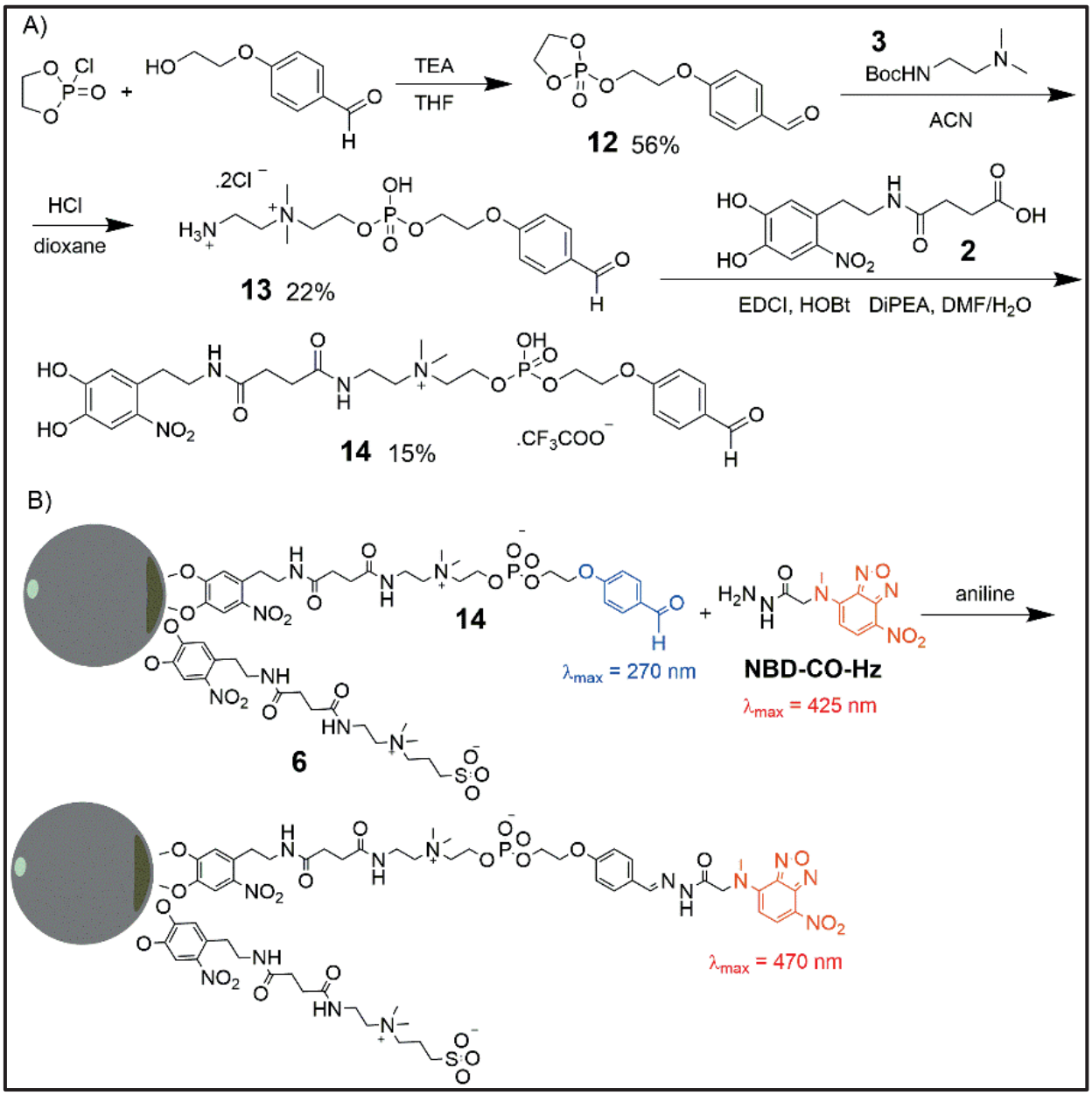

Figure 6. *A*) **Synthesis of zwitterionic aldehyde ligand 14.** *B*) **Bio-orthogonal hydrazone formation upon reaction between zwitterionic SPIONs and NBD-CO-H.**

425 nm in solution to 470 nm on the surface of the nanoparticles, which implies that NBD molecules experience a different environment on the nanoparticles. Also, by fluorescence we found an increased signal intensity of NBD as the aldehyde surface density is increased (*Figure S7*; NBD emits at 540 nm).

Conclusions

While aiming to develop systems-chemistry applications of SPIONs, we were unable to find protocols in the literature that enabled us to access stable dispersions of SPIONs in water that were amenable to dynamic covalent surface functionalization. This led us to investigate the stability of water-dispersed SPIONs coated by differently charged ligands (neutral, anionic,

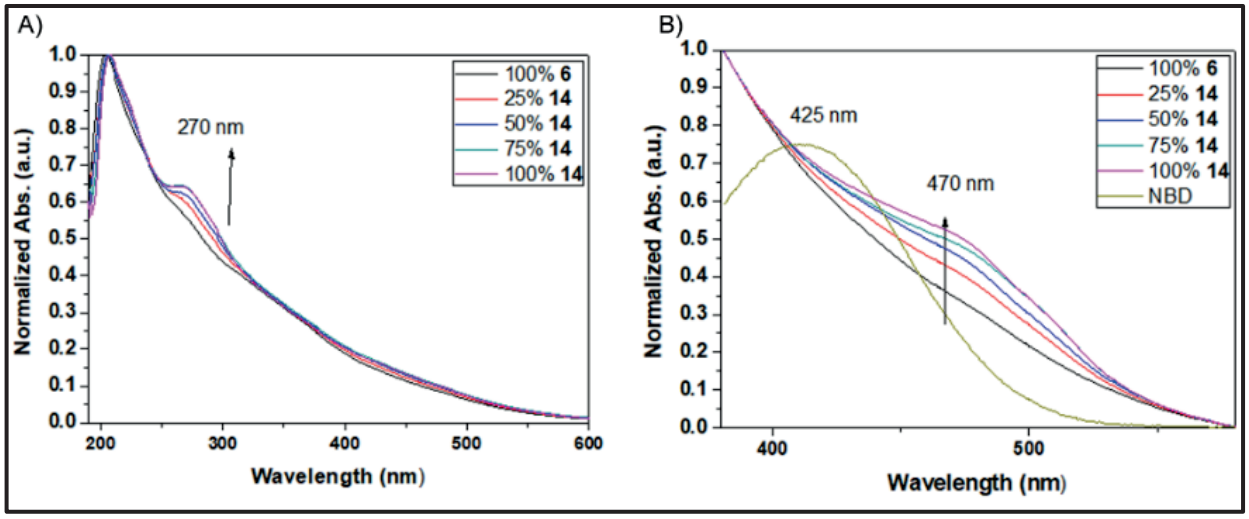

Figure 7. *A*) **UV spectra of zwitterionic NPs prepared using a mixture of zwitterionic ligand 6 and zwitterionic aldehyde 14 in different ratios.** *B*) **Normalized UV spectra of these zwitterionic NPs after hydrazone formation upon reaction with NBD-hydrazide** (λ_{max} = 425 nm)**, with the UV spectrum of the latter shown as well**. The ratios of **14/6** are: 0:100 (*black*); 25:75 (*red*); 50:50 (*blue*); 75:25 (*cyan*), and 100:0 (*purple*).

cationic and zwitterionic) across a range of pHs and ionic strengths. The results show that the zwitterionic ligands are most efficient at stabilizing the aqueous solutions of SPIONs, which remain well-dispersed for the entire 2-month period during which we monitored the samples. Furthermore, a zwitterionic ligand carrying an aldehyde group has been synthesized that allows, for the first time, for facile further dynamic covalent SPION surface modification and potentially also bioconjugation. The aldehyde can be grafted on the surface of the SPIONs at an arbitrary percentage of coverage and readily reacts with a hydrazide under mild condition. These results suggest that this SPION platform holds considerable promise for biological and biomedical studies and surface supported dynamic combinatorial chemistry for applications in systems chemistry [40].

Acknowledgements

We thank *Gang Ye* and *Victor Ivasyshyn* for TGA measurements, *Patricia Wolf* for proofreading. We are grateful for support from the *ERC*, *NWO*, the Ministry of Education, Culture and Science (Gravitation program 024.001.035), and the *China Scholarship Council*.

Author details

[1]Centre for Systems Chemistry, Stratingh Institute for Chemistry, University of Groningen, Nijenborgh 4, 9747 AG Groningen, The Netherlands.

[2]Stratingh Institute for Chemistry, University of Groningen, Nijenborgh 7, 9747 AG Groningen, The Netherlands.

[3]Current address for XM: Department of Organic Chemistry, Faculty of Chemistry, Weizmann Institute of Science, 234 Herzl Street, 7610001, Rehovot, Israel.

Author's contributions

X. M. and *P. N.* designed the experiments. X. M. and *N. E.* performed the experiments. *M. A.*, *G. I.*, and *I. M.* conducted the TEM measurements. *X. M.* drafted the manuscript. *S. O.*, *M. W.*, and *A. M.* wrote the final manuscript. All authors read and approved the final manuscript.

Competing interests

The authors declare that they have no competing interests.

Additional files

Additional file — Development of Stable Iron Oxide Nanoparticles for Dynamic Covalent Surface Functionalization

The additional file contains: *Figure S1-S7*, *Scheme S1*, and detailed experimental methods and characterization details of ligands and key intermediates.

References

1. Park, Y. I., Piao, Y., Lee, N., Yoo, B., Kim, B. H., Choi, S. H., Hyeon, T.: Transformation of hydrophobic iron oxide nanoparticles to hydrophilic and biocompatible maghemite nanocrystals for use as highly efficient MRI

contrast agent. J. Mater. Chem., 21, (2011), 11472 – 11477.

2. Wei, H., Bruns, O. T., Kaul, M. G., Hansen, E. C., Barch, M., Wiśniowska, A., Chen, O., Chen, Y., Li, N., Okada, S., Cordero, J. M., Heine, M., Farrar, C. T., Montana, D. M., Adam, G., Ittrich, H., Jasanoff, A., Nielsen, P., Bawendi, M. G.: Exceedingly small iron oxide nanoparticles as positive MRI contrast agents. Proc. Natl. Acad. Sci. U.S.A., 114, (2017), 2325 – 2330.
3. Kim, B. H., Lee, N., Kim, H., An, K., Park, Y. I., Choi, Y., Shin, K., Lee, Y., Kwon, S. G., Na, H. B., Park, J.-G., Ahn, T.-Y., Kim, Y.-W., Moon, W. K., Choi, S. H., Hyeon, T.: Large-scale synthesis of uniform and extremely small-sized iron oxide nanoparticles for high-resolution T1 magnetic resonance imaging contrast agents. J. Am. Chem. Soc., 133, (2011), 12624 – 12631.
4. Seo, W. S., Lee, J. H., Sun, X., Suzuki, Y., Mann, D., Liu, Z., Terashima, M., Yang, P. C., McConnell, M. V., Nishimura, D. G., Dai, H.: FeCo/graphitic-shell nanocrystals as advanced magnetic-resonance-imaging and near-infrared agents. Nat. Mater., 5, (2006), 971 – 976.
5. Kobayashi, T.: Cancer hyperthermia using magnetic nanoparticles. Biotechnol. J., 6, (2011), 1342 – 1347.
6. Bañobre-López, M., Teijeiro, A., Rivas, J.: Magnetic nanoparticle-based hyperthermia for cancer treatment. Rep. Pract. Oncol. Radiother., 18, (2013), 397 – 400.
7. Dave, S. R., Gao, X.: Monodisperse magnetic nanoparticles for biodetection, imaging, and drug delivery: a versatile and evolving technology. Wiley Interdiscip. Rev. Nanomed. Nanobiotechnol., 1, (2009), 583 – 609.
8. Beveridge, J. S., Stephens, J. R., Williams, M. E.: The use of magnetic nanoparticles in analytical chemistry. Annu. Rev. Anal. Chem., 4, (2011), 251 – 273.
9. Lee, H., Lee, E., Kim, D. K., Jang, N. K., Jeong, Y. Y., Jon, S.: Antibiofouling polymer-coated superparamagnetic iron oxide nanoparticles as potential magnetic resonance contrast agents for in vivo cancer imaging. J. Am. Chem. Soc., 128, (2006), 7383 – 7389.
10. Park, J., An, K., Hwang, Y., Park, J.-G., Noh, H.-J., Kim, J.-Y., Park, J.-H., Hwang, N.-M., Hyeon, T.: Ultra-large-scale syntheses of monodisperse nanocrystals. Nat. Mater., 3, (2004), 891 – 895.
11. Singh, G., Chan, H., Baskin, A., Gelman, E., Repnin, N., Král, P., Klajn, R.: Self-assembly of magnetite nanocubes into helical superstructures. Science, 345, (2014), 1149 – 1153.
12. Lynch, J., Zhuang, J., Wang, T., LaMontagne, D., Wu, H., Cao, Y. C.: Gas-bubble effects on the formation of colloidal iron oxide nanocrystals. J. Am. Chem. Soc., 133, (2011), 12664 – 12674.
13. Wei, H., Insin, N., Lee, J., Han, H.-S., Cordero, J. M., Liu, W., Bawendi, M. G.: Compact zwitterion-coated iron oxide nanoparticles for biological applications. Nano Lett., 12, (2012), 22 – 25.
14. Peng, S., Wang, C., Xie, J., Sun, S.: Synthesis and stabilization of monodisperse Fe nanoparticles. J. Am. Chem. Soc., 128, (2006), 10676 – 10677.
15. Amstad, E., Gillich, T., Bilecka, I., Textor, M., Reimhult, E.: Ultrastable iron oxide nanoparticle colloidal suspensions using dispersants with catechol-derived anchor groups. Nano Lett., 9, (2009), 4042 – 4048.
16. Liu, Y., Chen, T., Wu, C., Qiu, L., Hu, R., Li, J., Cansiz, S., Zhang, L., Cui, C., Zhu, G., You, M., Zhang, T., Tan, W.: Facile surface functionalization of hydrophobic magnetic nanoparticles. J. Am. Chem. Soc., 136, (2014), 12552 – 12555.
17. Morgese, G., Shirmardi Shaghasemi, B., Causin, V., Zenobi-Wong, M., Ramakrishna, S. N., Reimhult, E.; Benetti, E. M.: Next-generation polymer shells for inorganic nanoparticles are highly compact, ultra-dense, and long-lasting cyclic brushes. Angew. Chem. Int. Ed., 56, (2017), 4507 – 4511.
18. Gillich, T., Acikgöz, C., Isa, L., Schlüter, A. D., Spencer, N. D., Textor, M.: PEG-stabilized core–shell nanoparticles: impact of linear versus dendritic polymer shell architecture on colloidal properties and the reversibility of temperature-induced aggregation. ACS Nano, 7, (2013), 316 – 329.
19. Amstad, E., Gehring, A. U., Fischer, H., Nagaiyanallur, V. V., Hähner, G., Textor, M., Reimhult, E.: Influence of electronegative substituents on the binding affinity of catechol-derived anchors to Fe_3O_4 nanoparticles. J. Phys. Chem. C, 115, (2011), 683 – 691.
20. Lassenberger, A., Bixner, O.; Gruenewald, T., Lichtenegger, H., Zirbs, R., Reimhult, E.: Evaluation of high-yield purification methods on monodisperse PEG-grafted iron oxide nanoparticles. Langmuir, 32, (2016), 4259 – 4269.
21. Zürcher, S., Wäckerlin, D., Bethuel, Y., Malisova, B., Textor, M., Tosatti, S., Gademann, K.: Biomimetic surface modifications based on the cyanobacterial iron chelator anachelin. J. Am. Chem. Soc., 128, (2006), 1064 – 1065.
22. Wicklund, P. A., Brown, D. G.: Synthesis and characterization of some cobalt(III) catechol complexes. Inorg. Chem., 15, (1976), 396 – 400.
23. Grillo, V. A., Hanson, G. R., Wang, D., Hambley, T. W., Gahan, L. R., Murray, K. S., Moubaraki, B., Hawkins, C. J.: X-ray structural determination, and magnetic susceptibility, mössbauer, and EPR studies of $(Ph_4P)_2[Fe_2(Cat)_4(H_2O)_2]\cdot 6H_2O$, a catecholato-bridged dimer of iron(III). Inorg. Chem., 35, (1996), 3568 – 3576.
24. Lee, H., Scherer, N. F., Messersmith, P. B.: Single-molecule mechanics of mussel adhesion. Proc. Natl. Acad. Sci. U.S.A., 103, (2006), 12999 – 13003.
25. Ye, Q., Zhou, F., Liu, W.: Bioinspired catecholic chemistry for surface modification. Chem. Soc. Rev., 40, (2011), 4244 – 4258.
26. Rajh, T., Saponjic, Z., Liu, J., Dimitrijevic, N. M., Scherer, N. F., Vega-Arroyo, M., Zapol, P., Curtiss, L. A., Thurnauer, M. C.: Charge transfer across the nanocrystalline-DNA interface: Probing DNA recognition. Nano Lett., 4, (2004), 1017 – 1023.
27. Eisink, N. N. H. M., Lohse, J., Witte, M. D., Minnaard, A. J.: Regioselective oxidation of unprotected 1,4 linked glucans. Org. Biomol. Chem., 14, (2016), 4859 – 4864.
28. Martinez-Saez, N., Peregrina, J. M., Corzana, F.: Principles of mucin structure: implications for the rational design of cancer vaccines derived from MUC1-glycopeptides. Chem. Soc. Rev., 46, (2017), 7154 – 7175.
29. Gaidzik, N., Westerlind, U., Kunz, H.: The development of synthetic antitumour vaccines from mucin glycopeptide antigens. Chem. Soc. Rev., 42, (2013,) 4421 – 4442.
30. Boyer, C., Bulmus, V., Priyanto, P., Teoh, W. Y., Amal, R., Davis, T. P.: The stabilization and bio-functionalization of iron oxide nanoparticles using heterotelechelic polymers. J. Mater. Chem., 19, (2009), 111 – 123.

31. Mahdavi, M., Ahmad, M., Haron, M., Namvar, F., Nadi, B., Rahman, M., Amin, J.: Synthesis, surface modification and characterisation of biocompatible magnetic iron oxide nanoparticles for biomedical applications. Molecules, 18, (2013), 7533.
32. Yang, J., Cohen Stuart, M. A., Kamperman, M.: Jack of all trades: versatile catechol crosslinking mechanisms. Chem. Soc. Rev., 43, (2014), 8271 – 8298.
33. Avdeef, A., Sofen, S. R.; Bregante, T. L.; Raymond, K. N.: Coordination chemistry of microbial iron transport compounds. 9. Stability constants for catechol models of enterobactin. J. Am. Chem. Soc., 100,(1978), 5362 – 5370.
34. Holten-Andersen, N., Harrington, M. J.; Birkedal, H., Lee, B. P., Messersmith, P. B., Lee, K. Y. C., Waite, J. H.: pH-induced metal-ligand cross-links inspired by mussel yield self-healing polymer networks with near-covalent elastic moduli. Proc. Natl. Acad. Sci. U.S.A., 108, (2011), 2651 – 2655.
35. Zeng, H., Hwang, D. S., Israelachvili, J. N., Waite, J. H.: Strong reversible Fe^{3+}-mediated bridging between dopa-containing protein films in water. Proc. Natl. Acad. Sci. U.S.A., 107, (2010), 12850 – 12853.
36. Schlenoff, J. B.: Zwitteration: Coating surfaces with zwitterionic functionality to reduce nonspecific adsorption. Langmuir, 30, (2014), 9625 – 9636.
37. Stoneburner, S. J., Livermore, V., McGreal, M. E., Yu, D., Vogiatzis, K. D., Snurr, R. Q., Gagliardi, L.: Catechol-ligated transition metals: a quantum chemical study on a promising system for gas separation. J. Phys. Chem. C, 121, (2017), 10463 – 10469.
38. Zhan, N., Palui, G., Merkl, J.-P., Mattoussi, H.: Bio-orthogonal coupling as a means of quantifying the ligand density on hydrophilic quantum dots. J. Am. Chem. Soc., 138, (2016), 3190 – 3201.
39. Hu, G., Emrick, T.: Functional choline phosphate polymers. J. Am. Chem. Soc., 138, (2016), 1828 – 1831.
40. Corbett, P. T., Leclaire, J., Vial, L., West, K. R., Wietor, J.-L., Sanders, J. K. M., Otto, S.: Dynamic combinatorial chemistry. Chem. Rev., 106, (2006), 3652 – 3711.